Volume 1 | Number 1 | Jan 2013 | Pages 1–100

Journal of
Materials Chemistry C

Materials for optical and electronic devices
www.rsc.org/materialsC

ROYAL SOCIETY
OF CHEMISTRY

ROYAL SOCIETY
OF CHEMISTRY

www.rsc.org/materialsC

Journal Name

Synthesis, Characterization, and Physical Properties of Oligo(1-(*N*,*N*-dimethylamino)pyrrole)s and Their Doped Forms, Precursors of Candidates for Molecular Flat-band Ferromagnets
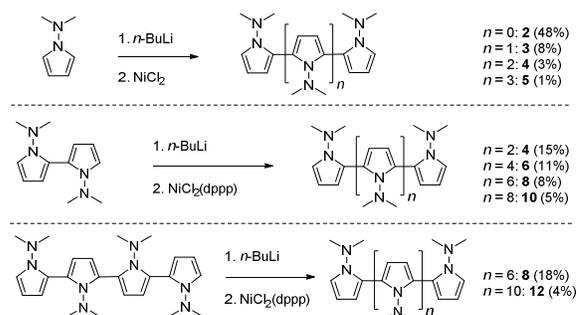
Yoshinori Yamanoi,* Kazuhiro Takahashi, Takeshi Hamada, Norikazu Ohshima, Masashi Kurashina, Yohei Hattori, Tetsuro Kusamoto, Ryota Sakamoto, Mariko Miyachi, and Hiroshi Nishihara*

Fully oxidized poly(1-(*N*,*N*-dimethylamino)pyrrole)s (PDMAPy^{n+}), which are synthesized through doping with anions with the same number of polymer units as the original pyrrole, have been proposed as candidates for molecular flat-band magnets from the theoretical calculations of Aoki and coworkers (*Phys. Rev. B*, 2003, **68**, 14040; *Phys. Rev. B*, 2010, **82**, 2235127). Here we describe the synthesis of neutral forms of oligo(1-(*N*,*N*-dimethylamino)pyrrole)s (ODMAPys) from the dimer (**2**) to the dodecamer (**12**). The crystal structures of **2**–**6** (i.e., up to the hexamer) were determined by single crystal X-ray analysis. The chemical and electrochemical formation of their oxidized forms is also reported. Electrochemical measurements of the ODMAPys indicated that oligomers **4**, **6**, and **8** underwent 2e$^−$ oxidation, whereas **10** and **12** showed quasi-reversible 4e$^−$ oxidation. The oxidized forms maintained considerable chemical stability; **4**$^{2+}$, **6**$^{2+}$, **8**$^{2+}$, **10**$^{4+}$, and **12**$^{4+}$ were isolated as SbCl$_6^−$ salts. The neutral forms were colorless (λ_{max} = 240–270 nm), whereas the oxidized forms exhibited strong blue color with λ_{max} = 670–950 nm. EPR spectroscopy indicated that the dications **4**$^{2+}$, **6**$^{2+}$, and **8**$^{2+}$ in the solid salts were intrinsically diamagnetic, but the tetracations of **10**$^{4+}$ were paramagnetic at 4.4 K, which was supported by magnetic measurements. These physical properties of the ODMAPys are different from those common to polypyrroles, but consistent with their predicted unique electronic structures.

1. Introduction

Polymers and oligomers with a π-conjugated system, so-called conducting polymers, have attracted considerable interest owing to their special redox and conductive properties and their applications as, for example, capacitors, batteries, electrochromic displays, OLEDs, and OFETs.[1-3] Particularly important are α,α-linked oligopyrroles, which are found in important conducting materials and also in some natural and medicinal products.[4-8] Such broad usefulness leads oligopyrroles bearing more elaborate substituents to be considered as promising candidates for organic electronic or optical materials.[9] Experimental and theoretical studies on the redox behaviors and electronic structures of the oxidized forms of unsubstituted oligopyrroles have been reported.[10-14] Aoki and coworkers predicted that the introduction of electron-donating substituents, such as NMe$_2$, would lead to significantly different properties in the oxidized forms; poly(1-(*N*,*N*-dimethylamino)pyrrole) (PDMAPy) and higher oligo(1-(*N*,*N*-dimethylamino)pyrrole) (ODMAPy) become flat-band ferromagnets when fully oxidized, namely when each pyrrole unit becomes a monocation.[15-18] Further calculations indicated that highly, but not fully, oxidized higher oligomers can form

ferromagnetic spin states, e.g., the octacations of the decamer and dodecamer.[19] This papers reports the first synthesis and characterization of ODMAPys from dimer to decamer and their oxidized forms. Combined electrochemical, UV–vis–NIR, and EPR studies were carried out to obtain detailed information on the stability and the unique electronic, optical, and magnetic properties of the oxidized forms.

Scheme 1 Synthesis of ODMAPys (**2**–**12**).

2. Results and Discussion

2.1 Synthesis, Characterization, and Structure of ODMAPy

The analysis in the present study requires several pure oligomers with different numbers of pyrrole units linked at the 2,5-positions in order to assess the effects of the number of pyrrole units on the oligomer structure and properties. Oligomers with controlled structures and degrees of polymerization were prepared not by oxidative polymerization but by sequential chemical synthesis.[20] Oligo(*N,N*-dimethylaminopyrrole)s (**2**–**12**) were prepared by successive lithiation and oxidative coupling reactions using a 2,2'-bi[1-(*N,N*-dimethylamino)pyrrole] starting material (Scheme 1). Of the Ni(II) and Cu(I) complexes tested for the coupling reaction, NiCl$_2$(dppp) gave the highest yield of the higher oligomers. High purity samples were obtained by preparative GPC to ensure monodispersity and the absence of contaminating homologues. We confirmed the existence of **7**, **9**, **11**, and higher oligomers, but we could not isolate them in their pure form. The structures of the oligomers were confirmed using ^{1}H NMR, ^{13}C NMR, EI- or FAB-MS, and elemental analysis.

The single-crystal X-ray structures of **2**, **3**, **4**, **5**, and **6** provided an insight into their solid-state structures (Figure 1). Important band distances (Å) and dihedral angles (deg) are described in this figure. Dimer **2** had two *N,N*-dimethylaminopyrrole rings inverted and on the same plane, indicating a fully π-conjugated structure. Higher oligomers (**3**–**6**) had the middle dimethylaminopyrrole ring inverted relative to the two outer rings; it was also inclined at 50°–80° to the less sterically hindered rings and at 90°–100° to the sterically hindered rings, which led to a loss of π-conjugation. Examination of C–C bond length between *N,N*-dimethylaminopyrrole rings indicated that the oligomerization had no effect on the bond lengths (changing the inter-ring C–C bond length by ≈ 0.02 Å). This is similar to C–C bond lengths of oligo(*N*-phenylpyrrole)s between pyrrole rings, which
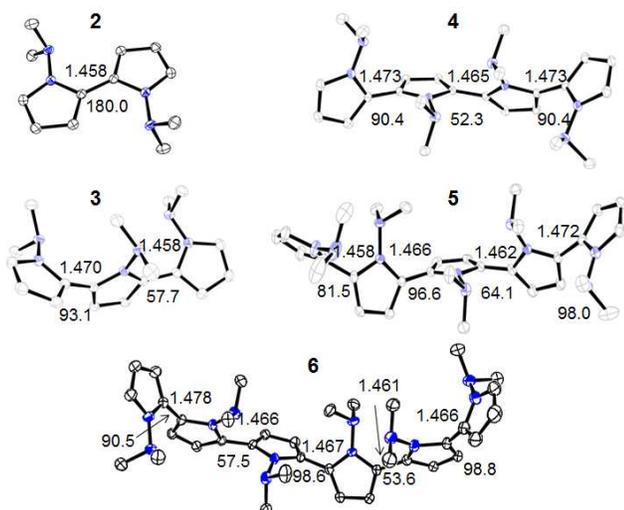

Fig. 2 UV–vis spectra of (a) ODMAPys in the neutral state and (b) vis–NIR spectra of their chemically oxidized forms, **4**$^{2+}$, **6**$^{2+}$, **8**$^{2+}$, **10**$^{4+}$, and **12**$^{4+}$ in SbCl$_6^-$ salts in CH$_3$CN. The right pictures are **4** and **4**$^{2+}$(SbCl$_6^-$)$_2$.

exhibited large dihedral angles.[21]

The UV–vis spectra of the ODMAPys (Figure 2(a)) show that increasing the oligomer length led to a smaller shift of the absorption maximum λ_{max} (nm) of the π–π* transition and of the molar extinction coefficient ε_{max} (M^{-1}cm^{-1}). Even the higher oligomers (e.g., **8** and **10**) showed λ_{max} < 270 nm, and were thus colorless, in contrast to regular polypyrroles. This small λ_{max} shift is attributed to a high torsion angle between the rings, which suggests steric hindrance arising from the substitution with an *N,N*-dimethylamino group.[22,23]

2.2 Redox Properties of ODMAPy

Cyclic voltammetry (CV) and differential pulse voltammetry (DPV) were carried out to examine the formation and stability of the oxidized forms of the ODMAPys. Note that the mono-mer, 1-(*N,N*-dimethylamino)pyrrole **1**, and its low oligomers (**2** and **3**) show only irreversible oxidation peaks in 0.1 M in *n*-Bu$_4$NClO$_4$-MeCN, indicating the considerable instability of the oxidized forms (Figure S1). The higher oligomers **4**, **6**, and **8** showed the first oxidation peak at ca. 0.05 V vs ferrocenium/ferrocene (Fc$^+$/Fc); the second peak was shifted to a less positive potential as their length increased from 1.15 V (**4**) to 0.65 V (**6**), and then to 0.30 V (**8**). When the potential was scanned to exceed the second oxidation peak, the oxidation peaks were irreversible at a scan rate of 0.1 Vs^{-1} (Figure 3, left). In contrast, scanning the potential within the range of the first oxidation peak led to reversible redox reactions (Figure 3, right). Coulometry at 0.6 V for **4**, at 0.3 V for **6**, and at 0.25 V for **8** showed n = 2.09, 2.01, and 2.02 electrons per molecule for the first oxidation wave, respectively, indicating 2e$^-$ oxidation (Figure S2). The difference between the anodic peak potential and the cathodic peak potential, ΔE_p, in the cyclic voltammogram for **4** was 107 mV, and the simulation gave E_1^o = 61 mV, E_2^o = 142 mV, and thus $E_2^o - E_1^o$ = 81 mV, which suggests two 1e$^-$ oxidations. However, ΔE_p = 38 and 40 mV for **6** and **8**, respectively; these values, which are slightly less than 57 mV, indicate a thermodynamically favorable one-step 2e$^-$ oxidation. The simulation gave E_1^o = 35 mV, E_2^o = 20 mV, and $E_2^o - E_1^o$ = −15 mV for **6**, and E_1^o = 38 mV, E_2^o = 9 mV, and

Fig. 1 ORTEP drawings showing 50% probability for **2**, **3**, **4**, **5**, and **6**. Numbers are C–C bond lengths (upper, Å) and dihedral angles (lower, degree) between two neighboring *N,N*-dimethylaminopyrrole rings.
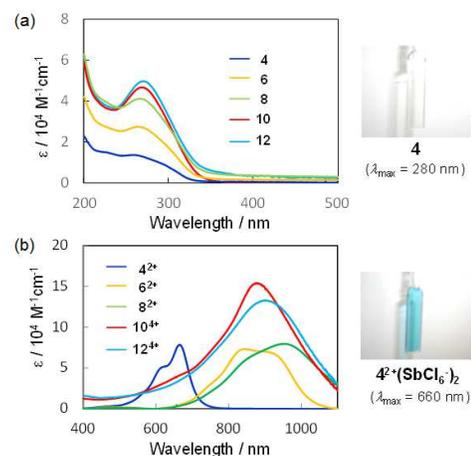
$E_2^{\circ} - E_1^{\circ} = -29$ mV for **8**, implying potential reversion (Figure S3).
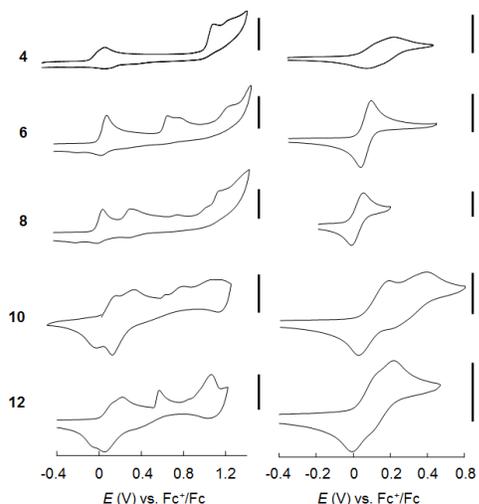

Fig. 3 Cyclic voltammograms of 1.0 mM ODMAPys (**4**, **6**, **8**, **10**, and **12**) in 0.1 M n-Bu$_4$NClO$_4$-CH$_3$CN at 100 mV s^{-1}. Scale bar is 40 μA.

The higher oligomers **10** and **12** showed different behaviors than the lower ones. Figure 2 shows their broad oxidation waves appearing between 0 and 0.6 V. These waves were chemically quasi-reversible when the potential scan was between −0.4 and 0.6 V for **10** and −0.4 and 0.5 V for **12**. Coulometry at 0.6 V for **10** and at 0.5 V for **12** gave $n = 4.05$ and 3.97, respectively, indicating 4e$^-$ oxidation. A potential scan for these oligomers to a larger positive potential of 1.2 V shows additional irreversible oxidation peaks. These results indicate that the highest oxidation states with considerable chemical stability were +2 for **4**, **6**, and **8** and +4 for **10** and **12**.

2.3 UV–vis–NIR spectra of the oxidized forms of ODMAPys: chemical oxidation and electrochemical oxidation

The oxidation potentials of ODMAPys are less positive than those of pyrrole because of the introduction of the electron-donating dimethylamino group.[24,25] The ODMAPys were oxidized using a small portion of the stoichiometric amount of (4-BrC$_6$H$_4$)$_3$NSbCl$_6$,[26-29] which has a reduction potential of 0.67 V vs Fc$^+$/Fc, in THF, and the UV–vis–NIR spectral changes were then measured (Figure S4). In most cases, the colorless solution turned a strong blue. We also carried out spectroelectrochemical measurements at a controlled potential in n-Bu$_4$NClO$_4$-MeCN (Figures S5 and S6), and the spectra were coincident with those obtained by the chemical oxidation. The UV–vis–NIR spectra of **4**$^{2+}$, **6**$^{2+}$, **8**$^{2+}$, **10**$^{4+}$ and **12**$^{4+}$ were extracted from the results obtained using the chemical oxidation method. The spectra are displayed in Figure 2b, and the λ_{max} and ε_{max} values are listed in Table 1. For the 2+ states, the λ_{max} value shifted greatly as the length of the oligomers increased from 650 nm for **4**$^{2+}$ to 950 nm for **8**$^{2+}$ compared with common polypyrrole derivatives, indicating the strong π-conjugation among the units in the oxidized states. The 4+ states of **10** and **12** gave λ_{max} around 900 nm, showing no further distinct red shift, although $\varepsilon_{max} = 1.54 \times 10^5$ and 1.33×10^5 M^{-1}cm^{-1},

respectively, which was about twice those of the 2+ states of the lower oligomers.

Color fading due to decomposition was observed in the MeCN solutions of the oxidized forms at room temperature. The stability of the **4**$^{2+}$, **6**$^{2+}$, and **8**$^{2+}$ states in MeCN under nitrogen at 298 K was examined via the change in their UV–vis–NIR spectra (Figure S7). The decomposition was via a first-order reaction, with the higher oligomers being substantially more stable than the shorter ones; $k_{dec} = 4.6 \times 10^{-3}$, 1.1×10^{-3}, and 5.6×10^{-5} s^{-1} for **4**$^{2+}$, **6**$^{2+}$, and **8**$^{2+}$, respectively, indicating that the oxidized species remained for 10 min, 90 min, and 10 h, respectively. Note that the tetracations **10**$^{4+}$ and **12**$^{4+}$ were much less stable in solution than the dications at room temperature. However, the decomposition was suppressed by decreasing the temperature, and the spectrum remained unchanged for several hours at 240 K in MeCN solution. It should also be mentioned that the powdered solid state of the oxidized forms was much more stable than the compounds in solution.

2.4 Synthesis and isolation of the oxidized forms of the ODMAPys

Based on the spectral data for chemical oxidation, the 2+ oxidized forms of **4**, **6**, and **8** were prepared by chemical oxidation using two equivalents of (4-BrC$_6$H$_4$)$_3$NSbCl$_6$ in THF for 10 min at room temperature under nitrogen. The resulting black precipitation was filtered and washed with THF and dichloromethane to give **4**$^{2+}$(SbCl$_6^-$)$_2$, **6**$^{2+}$(SbCl$_6^-$)$_2$, and **8**$^{2+}$(SbCl$_6^-$)$_2$ in moderate yields of 42%, 70%, and 61%, respectively. A similar method was used to synthesize **10**$^{4+}$(SbCl$_6^-$)$_4$, although the reaction temperature was 240 K in order to prevent the thermal decomposition of the oxidized product. Its thermal instability meant that the **10**$^{4+}$ samples were treated at low temperatures, and elemental analysis was not performed. However, its purity was checked using the UV–vis–NIR spectrum of the sample in MeCN. This is the first time that the 4+ oxidation state of an oligopyrrole derivative has been isolated.

2.5 Magnetic properties of the oxidized forms of ODMAPys

Theoretical calculations indicate that the oxidized species **4**$^{2+}$, **6**$^{2+}$, **8**$^{2+}$, and **10**$^{4+}$ have diamagnetic singlet ground states, whereas the energy difference be-tween the singlet and triplet states is small due to their unique electronic structures. The ^{1}H NMR spectra of the oxidized forms measured in CD$_2$Cl$_2$ did not show any sharp signals at room temperature, indicating that they are not purely diamagnetic. EPR spectra of the oxidized compounds were measured in the solid state at 4.6 or 4.2 K (Figure 4). Compounds **4**$^{2+}$, **6**$^{2+}$, and **8**$^{2+}$ each showed an extremely sharp isotropic signal at $g = 2.004$ with $\Delta T = 1.2$ mT, which is different from the signal of the oxidizing reagent ($g = 2.015$ and $\Delta T = 2.77$ mT). The spin density estimated from the integral of the signal using 2,2-diphenyl-1-picrylhydrazyl (DPPH) as a standard was quite small in each case (0.0005, 0.015, and 0.004 spin/molecule for **4**$^{2+}$, **6**$^{2+}$ and **8**$^{2+}$, respectively), indicating their intrinsically diamagnetic nature and quinoidal structure. Samples of **10**$^{4+}$(SbCl$_6^-$)$_4$ were carefully prepared and treated at low temperature (below 240 K) before the EPR measurement; its spectrum was measured at 4.4 K. In the solid state at 4.6 K, **10**$^{4+}$ also showed a sharp signal at $g = 2.003$ with $\Delta T = 1.2$ mT; the spin density of 0.42 is much higher than those of the dications of the lower oligomers. This significant difference is interesting, because common π-
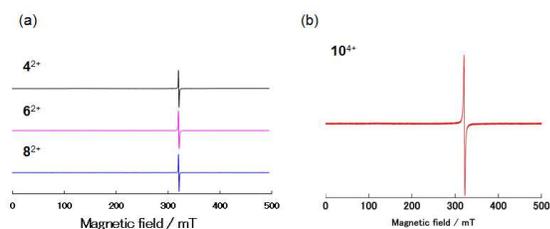
Fig. 4 (a) ESR spectra for 4^{2+}, 6^{2+}, and 8^{2+} in the solid state at 4.6 K. (b) ESR spectrum for 10^{4+} in the solid state at 4.2 K.
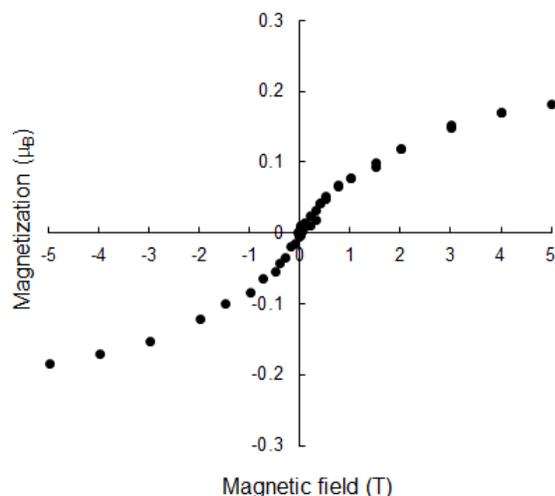

Fig. 5 Magnetic field dependence of magnetization of 10^{4+} at 2 K.

conjugated linear polymers, including polypyrroles, can form bipolarons to make the molecule diamagnetic in a highly doped state.[10-14] On the other hand, Aoki et al. proposed that a significant increase in the portion of the magnetic state is consistent with a decrease in the energy difference between high-spin and low-spin states upon higher doping. The high spin density on 10^{4+} relative to the negligible densities on 4^{2+}, 6^{2+}, and 8^{2+} suggests the possible occurrence of a flat-band ferromagnetism upon extended π-conjugation with higher hole doping. It should be noted that the EPR spectrum of 10^{4+} in MeCN glass at 4.4 K shows a similar sharp signal at $g = 2.003$, but the spin density was 0.032. This small value would be owing to the strong effects of the solvent molecules on the electronic properties, or to the shortened π-conjugation by the twisted molecular structure in the glass state.

The magnetization (M) of powder samples of 10^{4+} were measured using a SQUID magnetometer. The magnetic field dependence of the magnetization of 10^{4+} at 2 K is shown in Figure 5. Paramagnetic behavior is observed, and the spin density was estimated to be ca. 0.18 spin/molecule. This significant value is roughly in agreement with the EPR results.

3. Conclusions

Successive reductive coupling of dimethylaminopyrrole constitutes a practical and general approach to the synthesis of oligo(1-(*N,N*-dimethylamino)pyrrole)s (ODMAPys), which are candidate precursors for molecular flat-band magnets. The oxidation behaviors of ODMAPys were examined using electrochemical and UV–vis–NIR spectral measurements. The highest oxidation states with considerable stability are dications for teteramer **4**, hexamer **6**, and octamer **8** and teteracations for decamer **10** and dodecamer **12**. Upon oxidation, the absorption wavelength was more red-shifted compared with that observed for common polypyrroles. EPR spectroscopy indicated that 4^{2+}, 6^{2+}, and 8^{2+} are diamagnetic, whereas 10^{4+} is paramagnetic in the solid state at 4.6 K, a unique observation for oligopyrroles. Because oligo(1-(*N,N*-dimethylamino)pyrrole)s displayed high ring-torsional flexibility as shown in this study, this twist is large enough to prevent conjugation. Oligomers of five-membered aromatic heterocycles with highly coplanar conjugation should be designed to show flat-band ferromagnetism effectively. This opens a new possibility of functionalized materials in purely organic polymers.

Notes and references

Department of Chemistry, School of Science, The University of Tokyo, Hongo 7-3-1, Bunkyo-ku, Tokyo 113-0033, Japan. E-mail: yamanoi@chem.s.u-tokyo.ac.jp; nisihara@chem.s.u-tokyo.ac.jp

Electronic Supplementary Information (ESI) available: Molecular synthesis and structural characterization data, UV-Vis absorption and photooxidation details. See DOI: 10.1039/b000000x/

1   P. Bäuerle, *Adv. Mater.*, 1993, **5**, 879–886.

2   J.-M. Tour, *Chem. Rev.*, 1996, **96**, 537–554.

3   J. Roncali, *Chem. Rev.*, 1992, **92**, 711–738.

4   Magnetic Properties of Organic Materials; P. M. Lahti, Ed.; Marcel Dekker: New York, 1999; Vol. 279.

5   Molecular Magnetism: New Magnetic Materials; K. Itoh, M. Kinoshita, Eds.; Kodansha and Gordon & Breach: Tokyo and Amsterdam, 2000.

6   π-Electron Magnetism from Molecules to Magnetic Materials; J. Veciana, Ed.; Springer: Berlin, 2001.

7   Magnetism: Molecules to Materials V; J. S. Miller, M. Drillon, Eds.; Wiley-VCH: Weinheim, 2002.

8   S. Fox, H. Strasdeit, *Astrobiology*, 2013, **13**, 578–595.

9   U. Pfaff, A. Hildebrandt, D. Schaarschmidt, T. Rueffer, P. J. Low, H. Lang, *Organometallics*, 2013, **32**, 6106–6117.

10   Y. Dai, C. Wei, E. Blaisten-Barojas, *Comput. Theor. Chem.,* 2012, **993**, 7–12.

11   P.-C. Wang, J.-Y. Yu, *React. Funct. Polym.,* 2012, **72**, 311–316.

12   Y. Dai, E. J. Blaisten-Barojas, *Chem. Phys.,* 2008, **129**, 164903.

13   H. Liu, C. Yu, N. Gao, J. Zhao, *ChemPhysChem,* 2010, **11**, 1895–1902.

14   G. Zotti, S. Martina, G. Wegner, A. D. Schlueter, *Adv. Mater.*, 1992, **4**, 798–801.

15 R. Arita, Y. Suwa, K. Kuroki, H. Aoki, *Phys. Rev. B*, 2003, **68**, 140403.

16 R. Arita, Y. Suwa, K. Kuroki, H. Aoki, *Polyhedron*, 2003, **22**, 1883–1888.

17 Y. Suwa, R. Arita, K. Kuroki, H. Aoki, *Phys. Rev. B*, 2003, **68**, 174419.

18 R. Arita, Y. Suwa, K. Kuroki, H. Aoki, *Phys. Rev. Lett.*, 2002, **88**, 127202.

19 Y. Suwa, R. Arita, K. Kuroki, H. Aoki, *Phys. Rev. B*, 2010, **82**, 235127.

20 T. Yamamoto, H. Fukumoto, T. Koizumi, *J. Inorg. Organomet. Polym.*, 2009, **19**, 3–11.

21. U. Pfaff, A. Hildebrandt, D. Schaarschmidt, T. Rüffer, P. J. Low, H. Lang, *Organometallics*, 2013, **32**, 6106–6117.

22 T. Kauffmann, *Angew. Chem. Int. Ed.*, 1979, **18**, 1–19.

23 N. Rohde, E. U. Geisler, M. L. Hallensleben, B. Voigt, M. Voigt, *Adv. Mater.*, 1995, **7**, 401–404.

24 C. P. Andrieux, P. Hapiot, P. Audebert, L. Guyard, M. N. D. An, L. Groenendaal, E. W. Meijer, *Chem. Mater.*, 1997, **9**, 723–729.

25 G. Zotti, S. Martina, G. Wegner, A.-D. Schlüter, *Adv. Mater.*, 1992, 4, 798–801.

26 N. G. Connelly, W. E. Geiger, *Chem. Rev.*, 1996, **96**, 877–910.

27 F. A. Bell, A. Ledwith, D. C. Sherrington, *J. Chem. Soc. C*, 1969, 2719–2720.

28 Y. Matsuo, K. Tahara, E. Nakamura, *J. Am. Chem. Soc.*, 2006, **128**, 7154–7155.

29 R. Rathore, C. L. Burns, M. I. Deselnicu, *Org. Lett.*, 2001, **3**, 2887–2890.